Controllable Synthesis and Shape Evolution of PbTe Three-Dimensional Hierarchical Superstructures via an Alkaline Hydrothermal Method

Tie-Jun Zhu,* Xi Chen, Yi-Qi Cao, and Xin-Bing Zhao

State Key Laboratory of Silicon Materials, Department of Materials Science and Engineering, Zhejiang University, Hangzhou 310027, People's Republic of China

Received: January 15, 2009; Revised Manuscript Received: March 22, 2009

Symmetric hierarchical PbTe superstructures, including hopper cubes, flower-like structures, and dendritic structures, have been successfully fabricated by a facile alkaline hydrothermal method. Field emission scanning electron microscopy and transmission electron microscopy observations show that the PbTe hierarchical structures can be controlled by changing reaction temperature, reaction time, concentration of NaOH, and the kind of surfactants. The formation mechanism was investigated on the basis of the time-dependent experiment and the shape evolution. It is proposed that the formation of PbTe hopper cubic structures is due to the Berg effect induced concentration fluctuation of reactant ions, and the instability of growing fronts of crystals leads to the hierarchical dendritic morphologies. NaOH plays a crucial role in the formation stage. The Fourier transform infrared spectrum analysis showed that the band gap value of the PbTe hierarchical microcrystals was about 0.29 eV.

1. Introduction

Recently, materials with different sizes and morphologies have attracted more and more interest for their novel optical, electric, magnetic, and thermal properties and potential applications in nanoscale electronic and optoelectronic devices.[1] During the past few years, many efforts have been devoted to designing and synthesizing microcrystals and nanocrystals with specific sizes, shapes, and hierarchies using the so-called "bottom-up" approach.[2] Besides nanowires and nanotubes,[3] various materials with different morphologies have been reported, such as nanoribbons,[4] zigzag nanobelts,[5] helixlike structures,[6] and hierarchical dendrite structures.[7] Among them, the shape-controlled synthesis of complex three-dimensional (3D) architectures has been difficult to achieve and is a great challenge in the chemistry and materials area.[8]

Lead chalcogenides are very important narrow band gap semiconductors showing great promise in the fields of thermoelectric and infrared (IR) photoelectric devices.[9] Many recent studies on lead chalcogenides have been mainly focused on the controlled synthesis of different 3D structures, including PbTe dendritic structures,[10] PbTe spongelike structures,[11] PbSe octopod-like architectures,[12,13] PbS hierarchical structures,[14−16] PbS triangular nanopyramids,[17] PbS hyperbranched nanowire networks, and pine tree nanowires.[18−20] Various methods, such as electrochemical deposition,[10,21] sonochemistry,[11] alkaline etching method,[13] solvothermal method,[16,22] and chemical vapor transport,[18−20,23] have been used to produce them. These materials exhibit unique physical properties and should be of scientific and technological importance as building blocks for fabricating functional microdevices. For example, Li et al. studied the optical property of the PbTe dendritic structures and PbTe nanoparticles and found that the band gap of the former is higher.[10] Kerner et al. examined the thermal stability of PbTe spongelike structures and rectangular structures and observed a particular exothermal peak in the spongelike PbTe structures possibly due to a strain release process.[11]

Recently, Zhu et al. reported on complex PbTe hopper crystals with high hierarchy via the hydrothermal method,[24] which greatly stimulated the study of PbTe hierarchical architectures. However, to date, there are only limited reports on the preparation of lead chalcogenide hierarchical structures and the formation mechanism, which are relatively undeveloped and show some contrary results. For example, Zhang et al. fabricated PbTe hierarchical crystals using ethylene glycol as the solvent and PVP as the surfactant, suggesting that the capping effect of PVP is responsible for the formation of such structures.[25] Zhao et al. synthesized hierarchical PbS crystals using ethylenediamine as the solvent and concluded that ethylenediamine can cap {110} planes of nuclei more tightly.[26] Zhang et al. recently reported on PbSe hierarchical superstructures via a "top-down" etching route[13] and suggested that NaOH prefers to attack the {100} planes of PbSe cubes. More recently, Bierman et al. synthesized hierarchical PbS nanostructures of pine tree morphology by chemical vapor deposition, and a dislocation-driven growth mechanism was proposed.[20]

In this work, PbTe hierarchical superstructures, including hopper cubes, flower-like structures, and dendritic structures, have been synthesized via a simple alkaline hydrothermal process. Some factors affecting the morphologies of PbTe crystals, such as reaction time, temperature, concentration of NaOH, and surfactants, were systematically investigated. On the basis of the obtained results, a formation mechanism, different from those previously reported, of such hierarchical architectures is suggested, which is related to the Berg effect.[27] NaOH plays a crucial role in the formation of PbTe hierarchical superstructures with or without surfactants. In addition, the optical property of PbTe hierarchical structures was investigated by Fourier transform IR spectroscopy.

2. Experimental Section

Chemicals. All the chemicals used for the synthesis of PbTe hierarchical structures in this work are analytical grade without

* Corresponding author. Phone: 86-571-87952181. Fax: 86-571-87951451. E-mail: zhutj@zju.edu.cn.

10.1021/jp900452b CCC: $40.75
Published on Web 04/17/2009

further purification. $Pb(NO_3)_2$, Na_2TeO_3, and $NaBH_4$ were purchased from Shanghai Chemical Reagent Co. Ethanol, acetone, cetyl trimethyl ammonium bromide (CTAB), polyvinyl pyrrolidine (PVP), sodium dodecylbenzene sulfonate (SDBS), and NaOH were purchased from a variety of sources. Distilled water was obtained by a water-purification appliance.

Preparation of Hierarchical PbTe Structures. In a typical procedure, 0.12 mol of NaOH and 30 mL of distilled water were put into a beaker. The solution was stirred and heated to 100 °C, and NaOH was dissolved. Then, 3 mmol of Na_2TeO_3, 0.3 g of $NaBH_4$, and 3 mmol of $Pb(NO_3)_2$ were added in turn. After stirring for 5 min, the mixture was transferred into a 50 mL Teflon-lined stainless steel autoclave. The autoclave was held at 160 °C for 24 h and then cooled in air to room temperature. The gray powders were collected by filtering, washed with distilled water and ethanol, and finally air-dried for characterization. To study the growth mechanism and shape evolution process of the synthesized PbTe products, the effects of the synthesis conditions, such as reaction time, temperature, the concentration of NaOH, and the kind of surfactants (PVP, CTAB, and SDBS), were systematically investigated.

Characterization. The phase structure of the products was investigated by X-ray diffraction (XRD) on a Rigaku-D/MAX-2550PC diffractometer using Cu Kα radiation. The morphology and composition of the powders were analyzed by a Hitachi S-4800 field emission scanning electron microscope (FESEM) with energy-dispersive X-ray (EDX) spectrometer. Transmission electron microscopy (TEM), high-resolution TEM (HRTEM), and selected area electron diffraction (SAED) of the hierarchical superstructures were performed on a JEOL JEM-2010 microscope. The chemical states and the surface compositions of the synthesized PbTe powders were analyzed by X-ray photoelectron spectroscopy (XPS) on a RBD upgraded PHI-5000c ECSA system (PerkinElmer) with Mg Kα radiation ($h\upsilon = 1253.6$ eV) at an operating pressure of 5×10^{-8} Pa. The total power applied to the X-ray source was 250 W. Survey-scanning XPS spectra (0−1100 eV) and high-resolution spectra of Pb 4f, Te 3d, O 1s, and C 1s were both recorded by using RBD 147 interface (RBD Enterprises, USA) and the AugerScan 3.21 software. Binding energies were calibrated by using the containment carbon (C 1s = 284.6 eV). The data analyses were carried out by using the RBD AugerScan 3.21 software and XPSPeak4.1 software. The optical property of the products was performed with a Fourier transform infrared spectrometer (FTIR, Nicolet 5700). For analyses, the samples were prepared in the form of slices by mixing the product and KBr with a ratio of 1:20.

3. Results and Discussion

3.1. Structure and Morphology Characterization. Figure 1 shows the XRD pattern of the resulting powder obtained in 4 M NaOH at 160 °C for 24 h in the absence of any surfactant. All the diffraction peaks can be indexed to face-centered cubic (fcc) PbTe with space group $Fm\bar{3}m$ (225) (JCPDS: 38-1435), indicating that pure PbTe compound has been synthesized. The calculated lattice constant ($a = 6.464 \pm 0.017$ Å) is in good agreement with the standard literature value of 6.459 Å. The morphology of the PbTe powder was studied by FESEM. A low-magnification image is shown in Figure 2a, which indicates that the product mainly consists of 3D symmetric hierarchical crystals, including hopper cubes and flower-like structures. Figure 2b shows the high-magnification image of a hopper cube. It clearly reveals that each face of the cube has an inverse pyramid-shaped hole with {110} facets mostly exposed and the point of intersection of four {110} facets located at the center of the cube, whereas the {100} facets form the protruded terraces

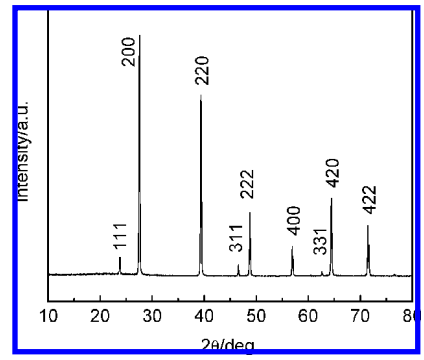

Figure 1. XRD pattern of PbTe powder synthesized by a hydrothermal method in 4 M NaOH at 160 °C for 24 h in the absence of any surfactants.

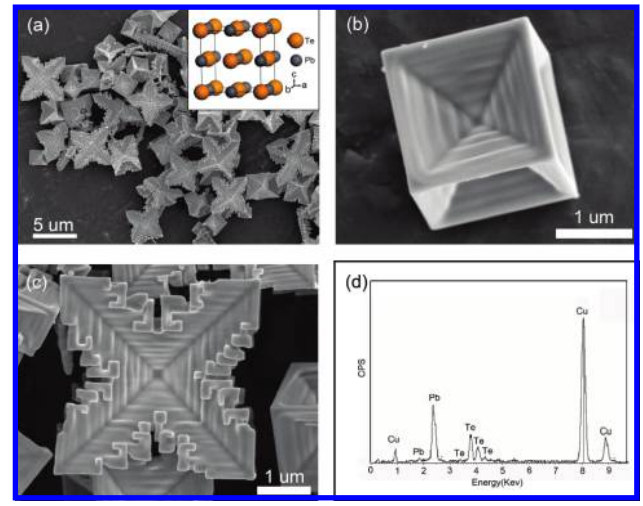

Figure 2. (a) Typical FESEM image of PbTe microcrystals. Inset: unit cell of PbTe (the smaller is Pb atoms). (b) Magnified image of a hopper cubic crystal. (c) Magnified image of a flower-like crystal. (d) EDX spectrum of PbTe microcrystals.

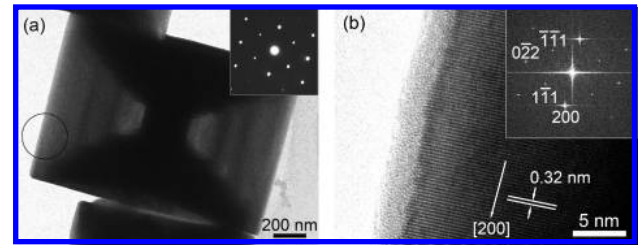

Figure 3. (a) TEM image of PbTe hopper cubic structure with the SAED pattern. (b) HRTEM image of the portion marked by the circle in (a). Inset: FFT of the lattice-resolved image.

on the side faces of the pyramid-shaped hole. Figure 2c shows a flower-like crystal, which is composed of eight hierarchical horns with high complexity. The star-shaped crystals with three tower-like horns can also be occasionally observed (Supporting Information, Figure S1). The composition of the product was checked by EDX analysis, as shown in Figure 2d. From the EDX spectrum, besides the Cu peak originating from the substrate, only lead and tellurium are found with the atomic ratio of about 1:1, agreeing well with the stoichiometric ratio of PbTe.

Panels a and b of Figure 3 are the TEM images of the hopper cubic structure to further present the detail of the product. The electron diffraction pattern in the low-magnification TEM image (Figure 3a) shows that the hopper cube is a single crystal. The high-resolution TEM image (Figure 3b) clearly shows that

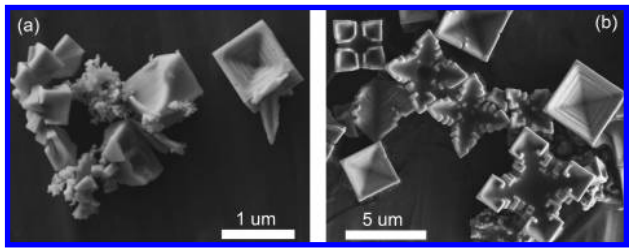

Figure 4. FESEM images of PbTe crystals synthesized in 4 M NaOH at (a) 100 °C and (b) 220 °C for 24 h in the absence of any surfactants.

the 2D lattice fringes are structurally uniform with the spacing of 0.32 nm, which is in good agreement with the *d* value of (200) planes of the fcc PbTe. The fast Fourier transform (FFT) of the lattice-resolved image (inset, Figure 3b) can be indexed to the [011] zone of a face-centered cubic PbTe, the same as that of the SAED in Figure 3a. From the HRTEM and FFT analyses, it can be deduced that the six facets of the crystal are along <100> directions and eight horns along <111> directions. Similar results have also been reported by other groups.[25] In addition, it can be seen that the surface of the particles is covered with a thin layer (2−3 nm) of amorphous material (Figure 3b), which is due to the oxidation of PbTe in air.[28,29]

3.2. Investigation of Influencing Factors. The factors affecting the morphology of PbTe crystals, including temperature, the concentration of NaOH, and the kind of surfactants, were systematically investigated. Temperature is one of the most important factors during the synthesis process. Therefore, the reactions were also carried out in 4 M NaOH while the temperature was reduced to 100 °C or raised to 220 °C for 24 h in the absence of any surfactant. Comparing the two FESEM images shown in Figure 4, one can find that product synthesized at the lower temperature (Figure 4a) has the smaller sizes (less than 1 μm) and incomplete hierarchical structures. When the reaction temperature was raised to 220 °C, the well-defined flower-like and hopper cubic structures with larger sizes (about 3−5 μm) were obtained, as shown in Figure 4b.

The concentration of NaOH is another important influencing factor. It was pointed out that there existed possibly a critical concentration of OH^-, and the quality of the target product was poor if the concentration was higher or lower.[24] Figure 5 shows the FESEM images of the products prepared with different OH^- concentrations at 160 °C for 24 h in the absence of any surfactant. When no NaOH was added, only PbTe particles were obtained, which have an average size of dozens of nanometers (Supporting Information, Figure S2). A trace of PbTe cubic hopper crystals can be observed with plenty of tiny PbTe nanoparticles when the concentration of NaOH is 1 M (Figure 5a). With increasing concentration of NaOH, more hopper cubes with bigger sizes are formed (Figure 5b). The well-defined hierarchical PbTe crystals can be obtained with the concentration of NaOH up to 4 M (Figure 5c). When the 8 M NaOH is used, the dendritic structures are well-developed (Figure 5d). The above fact shows that high concentrations of NaOH are favorable for the anisotropic growth of PbTe hierarchical crystals. NaOH may prefer to attack the {100} crystal planes and induce the surface energy rearrangement of PbTe nulei. It is worth mentioning that, when the PbTe cubic nanoparticles synthesized with no NaOH were again hydrothermally treated in 4 M NaOH at 160 °C for 24 h, no noticeable microstructural changes were observed (Supporting Information, Figure S3), indicating that NaOH should play its role during the nucleation and growth of PbTe crystals.

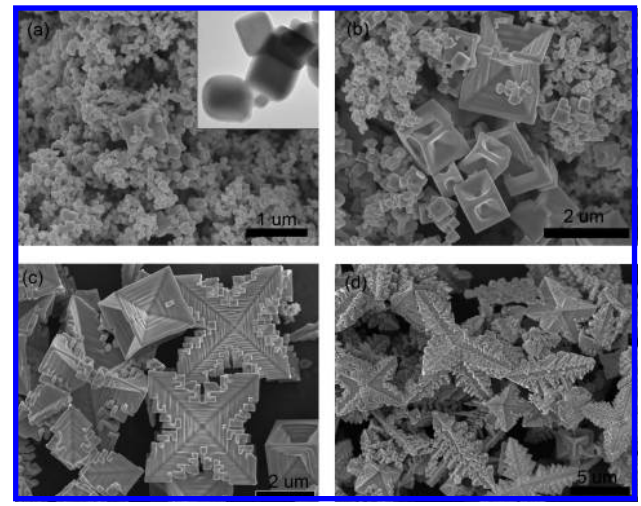

Figure 5. FESEM images of PbTe microcrystals synthesized with different concentrations of NaOH: (a) 1 M, (b) 2 M, (c) 4 M, and (d) 8 M. Inset: TEM image of cubic PbTe nanoparticles.

The chemical states and the surface compositions of the as-synthesized products were characterized by XPS. Figure 6 shows the XPS spectra taken from the products prepared in the solutions of 1 and 4 M NaOH, where the main products are cubic PbTe nanoparticles and hierarchical PbTe microcrystals, respectively. Figure 6a shows the XPS survey spectra of cubic and hierarchical PbTe. Only Pb, Te, C, and O peaks were found. The atomic ratios of Pb and Te are 12:11 for cubic and 4:3 for hierarchical PbTe. The lack of Te atoms in the latter should be due to the difference in shape of PbTe crystals. For the cubic PbTe nanoparticles, the exposed (100) facets contain an equal number of Pb and Te atoms, whereas the (110) facets of the hierarchical PbTe structures have more Pb than Te atoms. The high-resolution spectra of Pb 4f and Te 3d photoelectrons for cubic and hierarchical PbTe are shown in Figure 6b,c. The peak fitting of each high-resolution spectrum was achieved by the subtraction of a Shirley background, followed by the decomposition calculations using Lorentzian−Gaussian sum functions with a mixed parameter of 0.2.[30] As shown in Figure 5b, the Te $3d_{5/2}$ peak of both cubic and hierarchical structures can be decomposed into three peaks: 572.1(572.2), 574.6(574.7), and 576.1(576.3) eV, respectively, corresponding to the three chemical binding states of PbTe,[29] $PbTeO_3$, and TeO_2.[31,32] The chemical binding state at about 574.6 eV has rarely been found in the previous reports on PbTe crystals, and we ascribed it to the oxidized thin surface layer. As shown in Figure 5c, the Pb $4f_{7/2}$ peak of cubic PbTe is decomposed to two peaks at 137.1 and 138.2 eV, corresponding to the expected chemical shift for PbTe and PbO, respectively.[33] The Pb $4f_{7/2}$ peak of the hierarchical PbTe can be fitted into 137.2 and 138.7 eV peaks, respectively, which proves the existence of PbTe and $Pb(OH)_2$ and is in good agreement with the previous report.[34] Figure 6d shows the high-resolution spectra of O 1s photoelectrons for cubic PbTe nanoparticles and hierarchical PbTe superstructures. The O 1s peaks of both structures can be decomposed to two peaks: 530.7(530.3) and 528.8(528.3) eV, which correspond to the chemical binding states of adsorption oxygen and oxides of Pb and Te.[35] To sum up, no elemental Pb and Te were detected in the synthsized products. The surface chemical states and compositions between cubic and hierarchical PbTe are different due to the different shapes of the products. In high concentrations of NaOH, Pb is more easily oxidized into $Pb(OH)_2$.

Surfactants can also play an obvious role in the morphology of the products. The preferential adsorption of surfactant

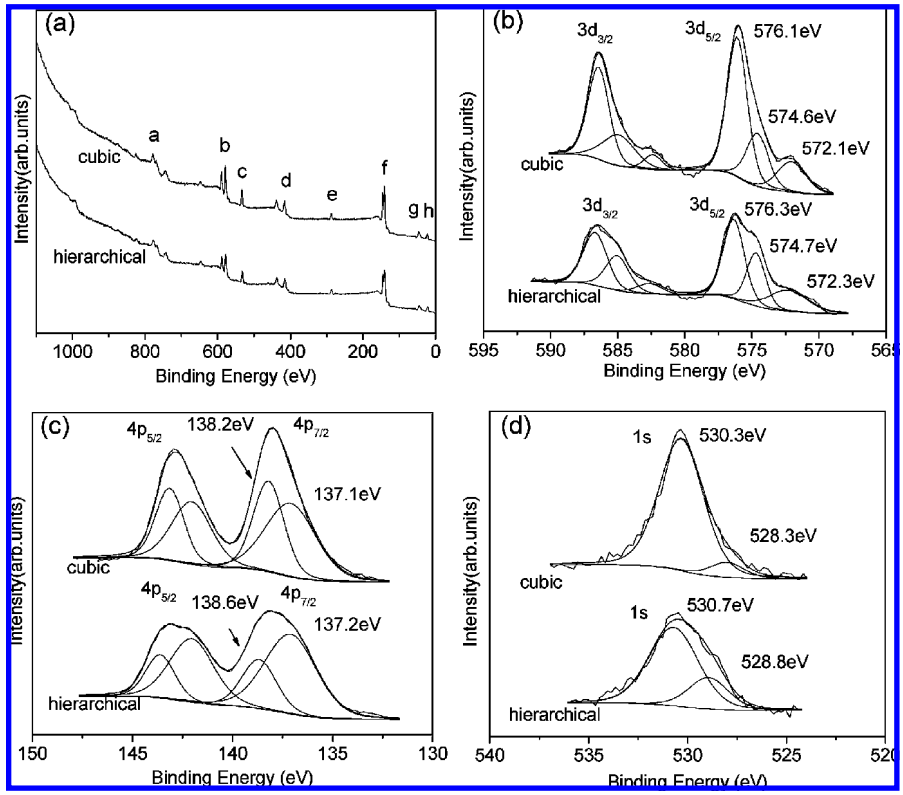

Figure 6. (a) XPS survey spectra of cubic PbTe nanoparticles and hierarchical PbTe microstructure products: a, Te MNN; b, Te 3d5; c, O 1s; d, Pb 4d5; e, C 1s; f, Pb 4f7; g, Te 4d5; h, Pb 5d5. High-resolution spectra of (b) Te 3d, (c) Pb 4f, and (d) O 1s photoelectrons for cubic PbTe nanoparticles and hierarchical PbTe superstructures.

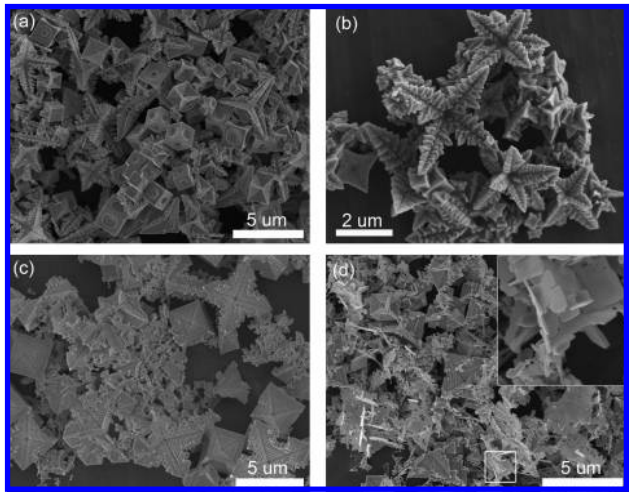

Figure 7. FESEM images of PbTe products in the presence of different surfactants: (a) CTAB, (b) PVP, and (c) SDBS at 160 °C for 24 h. (d) FESEM image of PbTe products synthesized with SDBS at 160 °C for 48 h. Inset: the magnification of the area marked by the square.

molecules on different crystal faces may direct the growth of particles into various shapes by controlling the growth rates along the different crystal axes. Figure 7a is the SEM image of the as-synthesized product in 4 M NaOH at 160 °C for 24 h in the presence of CTAB. It indicates that the product consists of the flower-like structures and the hopper cubes with a round hole at the center of each face. With increasing reaction time to 48 h, the almost same products with the flower-like and hopper cubic structures were obtained (Supporting Information, Figure S4), indicating that CTAB may inhibit the growth of hierarchical flower-like structures. One-dimensional PbTe nanowires have been synthesized by a CTAB-assisted hydrothermally

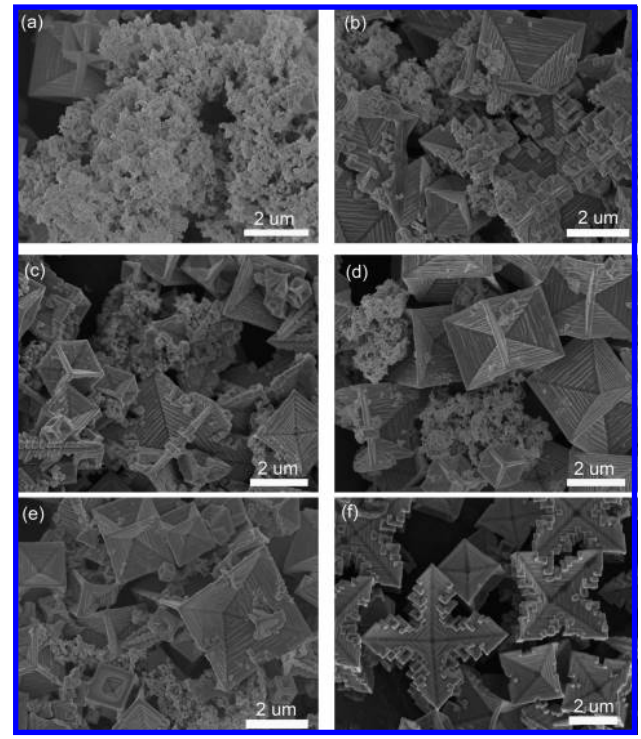

Figure 8. FESEM images of the PbTe crystals synthesized in 4 M NaOH at 160 °C for different time intervals: (a) 3, (b) 6, (c) 9, (d) 12, (e) 18, and (f) 24 h.

driven rolling up process,[36,37] where CTAB was considered to act as an etchant beneficial for producing 1D structures. However, in this work, CTAB should act as the stabilizing agent and is favorable for the formation of cubic PbTe crystals. Figure 7b shows that dendritic structures with eight identical tower-

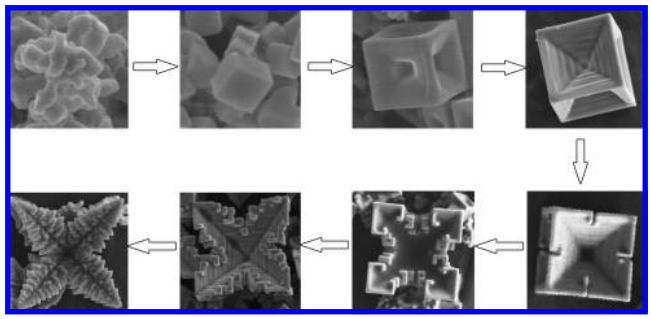

Figure 9. Formation process of PbTe hierarchical microstructures.

like horns were synthesized using PVP as the surfactant. Zhang et al.[25] also reported such an architecture using ethylene glycol as the solvent and PVP as the surfactant, which actually acted as the capping agent. The role of PVP in our experiment is considered to be same. The adsorption and desorption of PVP molecules on different faces of PbTe nuclei may kinetically control the growth rates along different crystal directions. Figure 7c is the SEM image of PbTe crystals using SDBS as the surfactant, showing that the product consists of submicron particles, hopper cubes, and flower-like structures. Prolonging the reaction time to 48 h, a large amount of nanosheets was observed, as shown in Figure 7d. The nanosheets have a thickness of 20−50 nm. Zhu et al.[24] suggested that the addition of SDBS to the solution resulted in the formation of more dendritic structures and pointed out that SDBS acted as a capping agent. In this work, however, different results were obtained. SDBS molecules seem to absorb onto some surfaces of PbTe crystals, leading to highly anisotropic growth of PbTe crystals. All in all, surfactants do play an important role in influencing the morphology of the synthesized PbTe products. However, the flower-like hierarchical structure can be found in all the products even when using different kinds of surfactants, which indicates that surfactants may not be the crucial factor for the formation of such a flower-like superstructure in the solution with high concentrations of NaOH. The interaction between surfactant molecules and PbTe nuclei can be weakened due to the role of OH^-.

3.3. Time-Dependent Experiment and the Growth Mechanism. To obtain a better understanding of the growth mechanism of hierarchical PbTe crystals, a time-dependent experiment was carried out at 160 °C for 3, 6, 9, 12, and 18 h with 4 M NaOH in the absence of any surfactant. The shape evolution of the synthesized PbTe crystals is shown in Figure 8. When the reaction time is 3 h, the main product is PbTe nanoparticles and a few hopper cubic structures are occasionally found (Figure 8a). Both the hopper structures and the nanoparticles are produced after 6 h (Figure 8b). Prolonging the reaction time to 9 h, more nanoparticles transform to hopper cubes (Figure 8c). As the reaction time further increases, the cubes grow bigger and the number of nanoparticles decreases gradually (Figure 8d,e). For a reaction time of 24 h, 3D well-defined symmetric hierarchical PbTe dendritic architectures were obtained (Figure 8f).

The formation of PbTe hierarchical structures should be determined by the nucleation and the subsequent growth stage. The growth process proceeds according to the crystal habit and to the branching process, which are associated with the energy of the exposed facets (kinetics) and the diffusion effect, respectively. During the nucleation, PbTe seeds crystallize as polyhedrons, which expose six {100} planes and eight {111} planes due to their highly symmetric cubic rocksalt crystal structures.[38] Then at the growth stage, the shape evaluation of crystals is determined by the ratio of the growth rate in the [100] to that in the [111].[39] As an fcc crystal, {111} planes have higher energy than {100} ones and, hence, a faster growth rate along [111] direction than along [100] direction. Thus, an fcc crystal can naturally grow into a cubic structure with {100} facets exposed, as shown in Figure 5a. Interestingly, the hierarchical PbTe superstructures were obtained only in the presence of NaOH, regardless of the presence of any surfactants. We propose that, therefore, NaOH plays a crucial role in the formation of PbTe hierarchical superstructures. Similar hierarchical architectures have also been found in various compounds, such as $CaCO_3$,[40] Cu_2O,[41] MoS_2,[42] and $Ba(NO_3)_2$.[43] They were obtained by changing certain experimental conditions, such as solvents (gel media[40] and alkaline microemulsion[41]), concentration of precursors,[42,43] and voltage,[44] which can obviously affect the diffusion process. As to the formation of PbX (X = S, Se, Te) hierarchical structures by wet chemical methods, there are two main mechanisms previously reported: capping effect of solvent[26] or surfactant[25] and etching effect of OH^-.[13] However, these two mechanisms cannot explain why the hopper holes initially occur at the center of each facet. It is known that the morphology of crystals strongly depends on the deviation of the formation conditions from the thermodynamic equilibrium.[43,44] Near the equilibrium conditions, specific polyhedral forms are created through a kinetic-controlled reaction and the surface energy will take a minimum value. With increasing the driving force of crystallization, skeletal crystals are produced. Under far-equilibrium conditions, the instability of the growing fronts of crystals leads to the formation of dendritic morphology due to the increased contribution of mass or heat diffusion. On the basis of our experimental results and the above discussion, we

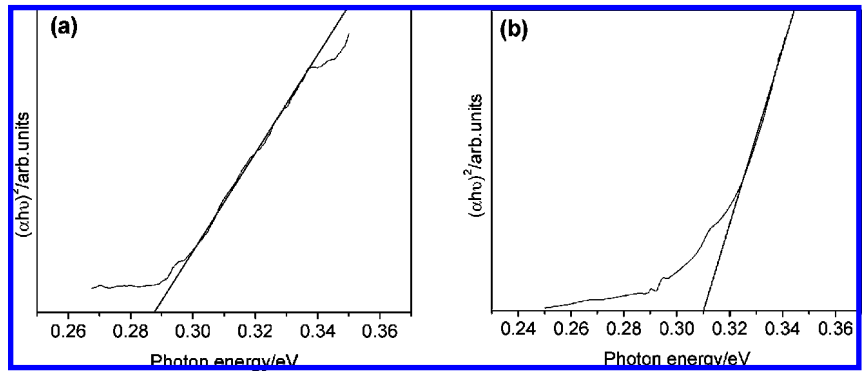

Figure 10. Plot of $(\alpha h\nu)^2$ vs $h\nu$ for determination of the band gap of (a) PbTe hierarchical structures synthesized in 4 M NaOH at 160 °C for 24 h in the absence of any surfactant and (b) PbTe nanoparticles synthesized without NaOH.

consider that the morphological evolution process of PbTe hierarchical structures can be illustrated in Figure 9. First, PbTe nuclei form, which is controlled by kinetics. The cubes are formed due to the high energy of the {111} facets. It is well-known that, when a crystal is polyhedral with smooth interfaces, the concentration of reaction ions over a face is not uniform: it is higher near the edges and corners than at the center of a face, which is named the Berg effect.[27,45] Therefore, when the growth of PbTe cubes proceeds, the process will be controlled by the Berg effect. The concentration of Pb and Te ions is higher at the edges and corners, which is favorable for the formation of new layers at the edges of the {100} faces. Thus, the hopper cubic structure is formed, and these structures grow along the <111> direction. NaOH is necessary in synthesizing PbTe hierarchical superstructures, which may greatly strengthen the Berg effect. With increasing reaction time, the new layers are formed at the eight corners and caused a gap in the middle of each edge. The instability of the growing fronts finally leads to the formation of the dendritic structures.

3.4. Optical Property of PbTe Hierarchical Structures. The optical property of PbTe hierarchical crystals synthesized in 4 M NaOH at 160 °C for 24 h was studied by an FTIR spectrometer in the spectral range of 2.5−25 μm at room temperature. The FTIR spectrum for the PbTe nanoparticles of ~40 nm synthesized at 160 °C for 24 h without NaOH (Supporting Information, Figure S2) was also carried out for comparison. Figure 10 shows the plot of $(\alpha h\nu)^2$ versus photon energy ($h\nu$) for the PbTe hierarchical structures and the PbTe nanoparticles. The band gap value (E_g) can be calculated by extending the linear part of the curve to zero absorption. The band gap value of the PbTe hierarchical structure was estimated to be about 0.29 eV, which is in good agreement with literature values.[10,46,47] For the PbTe nanoparticles, the band gap values shifted to 0.31 eV, which is higher than that of the PbTe hierarchical microcrystals due to the strong quantum confinement effect.[48]

4. Conclusion

Hierarchical PbTe structures, such as hopper cubic, flower-like, and dendritic structures, have been successfully synthesized by a facile alkaline hydrothermal method. The influencing factors, including reaction temperature and time, concentration of NaOH, and the kind of surfactants, were systematically investigated. It is suggested that the formation of hierarchical PbTe structures is due to the deviation of the formation conditions from the thermodynamic equilibrium, and hopper cubic structures are formed due to the nonuniformity of the solute distribution (Berg effect) over the crystal faces. NaOH plays a crucial role in the formation process. The band gap value of hierarchical PbTe structures was calculated to be about 0.29 eV from the FTIR absorption spectrum.

Acknowledgment. The work is financially supported by the National "863" Hi-tech R&D Program of China (2007AA03Z234), the National "973" Basic Research Program (2007CB607502), and the Natural Science Foundation of China (50601022).

Supporting Information Available: FESEM images of PbTe crystals and nanoparticles. This material is available free of charge via the Internet at http://pubs.acs.org.

References and Notes

(1) Xia, Y. N.; Yang, P. D.; Sun, Y. G.; Wu, Y. Y.; Mayers, B.; Gates, B.; Yin, Y. D.; Kim, F.; Yan, Y. Q. *Adv. Mater.* **2003**, *15*, 353. Kuang, D. B.; Xu, A. W.; Fang, Y. P.; Liu, H. Q.; Frommen, C.; Fenske, D. *Adv. Mater.* **2003**, *15*, 1747.

(2) Duan, X. F.; Huang, Y.; Cui, Y.; Wang, J. F.; Lieber, C. M. *Nature* **2001**, *409*, 66. Hu, J. T.; Odom, T. W.; Lieber, C. M. *Acc. Chem. Res.* **1999**, *32*, 435.

(3) Cui, Y.; Lieber, C. M. *Science* **2001**, *291*, 851. Kong, J.; Franklin, N. R.; Zhou, C. W.; Chapline, M. G.; Peng, S.; Cho, K. J.; Dai, H. J. *Science* **2000**, *287*, 622.

(4) Li, X. L.; Wang, X. R.; Zhang, L.; Lee, S. W.; Dai, H. J. *Science* **2008**, *319*, 1229. Gao, P. X.; Ding, Y.; Mai, W. J.; Hughes, W. L.; Lao, C. S.; Wang, Z. L. *Science* **2005**, *309*, 1700.

(5) Duan, J. H.; Yang, S. G.; Liu, H. W.; Gong, J. F.; Huang, H. B.; Zhao, X. N.; Zhang, R.; Du, Y. W. *J. Am. Chem. Soc.* **2005**, *127*, 6180.

(6) Liu, B.; Yu, S. H.; Li, L. J.; Zhang, Q.; Zhang, F.; Jiang, K. *Angew. Chem., Int. Ed.* **2004**, *43*, 4745.

(7) Cao, H. L.; Gong, Q.; Qian, X. F.; Wang, H. L.; Zai, J. T.; Zhu, Z. K. *Cryst. Growth Des.* **2007**, *7*, 425.

(8) Narayanaswamy, A.; Xu, H. F.; Pradhan, N.; Kim, M.; Peng, X. G. *J. Am. Chem. Soc.* **2006**, *128*, 10310.

(9) Harman, T. C.; Taylor, P. J.; Walsh, M. P.; LaForge, B. E. *Science* **2002**, *297*, 2229.

(10) Li, G. R.; Yao, C. Z.; Lu, X. H.; Zheng, F. L.; Feng, Z. P.; Yu, X. L.; Su, C. Y.; Tong, Y. X. *Chem. Mater.* **2008**, *20*, 3306.

(11) Kerner, R.; Palchik, O.; Gedanken, A. *Chem. Mater.* **2001**, *13*, 1413.

(12) Wang, X. Q.; Xi, G. C.; Liu, Y. K.; Qian, Y. T. *Cryst. Growth Des.* **2008**, *8*, 1406.

(13) Zhang, S. D.; Wu, C. Z.; Wu, Z. C.; Yu, K.; Wei, J. B.; Xie, Y. *Cryst. Growth Des.* **2008**, *8*, 2933.

(14) Zhang, Z. H.; Lee, S. H.; Vittal, J. J.; Chin, W. S. *J. Phys. Chem. B* **2006**, *110*, 6649.

(15) Bakshi, M. S.; Thakur, P.; Sachar, S.; Kaur, G.; Banipal, T. S.; Possmayer, F.; Petersen, N. O. *J. Phys. Chem. C* **2007**, *111*, 18087.

(16) Zuo, F.; Yan, S.; Zhang, B.; Zhao, Y.; Xie, Y. *J. Phys. Chem. C* **2008**, *112*, 2831.

(17) Wang, C. W.; Liu, H. G.; Bai, X. T.; Xue, Q. B.; Chen, X.; Lee, Y. I.; Hao, J. C.; Jiang, J. *Cryst. Growth Des.* **2008**, *8*, 2660.

(18) Ge, J. P.; Wang, J.; Zhang, H. X.; Wang, X.; Peng, Q.; Li, Y. D. *Chem.—Eur. J.* **2005**, *11*, 1889.

(19) Bierman, M. J.; Lau, Y. K. A.; Jin, S. *Nano Lett.* **2007**, *7*, 2907.

(20) Bierman, M. J.; Lau, Y. K. A.; Kvit, A. V.; Schmitt, A. L.; Jin, S. *Science* **2008**, *320*, 1060.

(21) Xiao, F.; Yoo, B.; Bozhilov, K. N.; Lee, K. H.; Myung, N. V. *J. Phys. Chem. C* **2007**, *111*, 11397.

(22) Zhang, C.; Kang, Z. H.; Shen, E. H.; Wang, E. B.; Gao, L.; Luo, F.; Tian, C. G.; Wang, C. L.; Lan, Y.; Li, J. X.; Cao, X. J. *J. Phys. Chem. B* **2006**, *110*, 184.

(23) Zhu, J.; Peng, H. L.; Chan, C. K.; Jarausch, K.; Zhang, X. F.; Cui, Y. *Nano Lett.* **2007**, *7*, 1095.

(24) Zhu, J. P.; Yu, S. H.; He, Z. B.; Jiang, J.; Chen, K.; Zhou, X. Y. *Chem. Commun.* **2005**, 5802.

(25) Zhang, G.; Lu, X.; Wang, W.; Li, X. *Chem. Mater.* **2007**, *19*, 5207.

(26) Zhao, P. T.; Wang, J. M.; Cheng, G.; Huang, K. X. *J. Phys. Chem. B* **2006**, *110*, 22400.

(27) Berg, W. L. *Proc. R. Soc. London, Ser. A* **1937**, *164*, 79.

(28) Yashina, L. V.; Kobeleva, S. P.; Neudachina, V. S.; Shatalova, T. B.; Zlomanov, V. P. XPS Study of Fresh and Oxidized (Pb,Ge)Te Surfaces. *9th European Conference on Applications of Surface and Interface Analysis*, Avignon, France, 2001.

(29) Yashina, L. V.; Tikhonov, E. V.; Neudachina, V. S.; Zyubina, T. S.; Chaika, A. N.; Shtanov, V. I.; Kobeleva, S. P.; Dobrovolsky, Y. A. The Oxidation of PbTe(100) Surface in Dry Oxygen. *10th European Conference on Applications of Surface and Interface Analysis (ECASIA 03)*, Berlin, Germany, 2003.

(30) Zhu, T. J.; Lu, L. *J. Appl. Phys.* **2004**, *95*, 241.

(31) Song, J. M.; Lin, Y. Z.; Zhan, Y. J.; Tian, Y. C.; Liu, G.; Yu, S. H. *Cryst. Growth Des.* **2008**, *8*, 1902.

(32) Menke, E. J.; Brown, M. A.; Li, Q.; Hemminger, J. C.; Penner, R. M. *Langmuir* **2006**, *22*, 10564.

(33) Zyubina, T. S.; Neudachina, V. S.; Yashina, L. V.; Shtanov, V. I. *Surf. Sci.* **2005**, *574*, 52.

(34) Yang, Y.; Kung, S. C.; Taggart, D. K.; Xiang, C.; Yang, F.; Brown, M. A.; Guell, A. G.; Kruse, T. J.; Hemminger, J. C.; Penner, R. M. *Nano Lett.* **2008**, *8*, 2447.

(35) Yashina, L. V.; Puettner, R.; Zyubina, T. S.; Poygin, M.; Shtanov, V. I.; Neudachina, V. S.; Molodtsov, S. L.; Dobrovolsky, Y. A. *J. Phys. Chem. C* **2007**, *111*, 17297.

(36) Qiu, X. F.; Lou, Y. B.; Samia, A. C. S.; Devadoss, A.; Burgess, J. D.; Dayal, S.; Burda, C. *Angew. Chem., Int. Ed.* **2005**, *44*, 5855.

(37) Zhang, L. Z.; Yu, J. C.; Mo, M. S.; Wu, L.; Kwong, K. W.; Li, Q. *Small* **2005**, *1*, 349.

(38) Lee, S. M.; Jun, Y. W.; Cho, S. N.; Cheon, J. *J. Am. Chem. Soc.* **2002**, *124*, 11244. Lu, W. G.; Fang, J. Y.; Stokes, K. L.; Lin, J. *J. Am. Chem. Soc.* **2004**, *126*, 11798. Cho, K. S.; Talapin, D. V.; Gaschler, W.;

Murray, C. B. *J. Am. Chem. Soc.* **2005**, *127*, 7140. Mokari, T. L.; Zhang, M. J.; Yang, P. D. *J. Am. Chem. Soc.* **2007**, *129*, 9864. Tai, G.; Zhou, B.; Guo, W. L. *J. Phys. Chem. C* **2008**, *112*, 11314.

(39) Sun, Y. G.; Xia, Y. N. *Science* **2002**, *298*, 2176. Bashouti, M.; Lifshitz, E. *Inorg. Chem.* **2008**, *47*, 678.

(40) Yang, D.; Qi, L. M.; Ma, J. M. *Chem. Commun.* **2003**, 1180.

(41) Zhang, H. W.; Zhang, X.; Li, H. Y.; Qu, Z. K.; Fan, S.; Ji, M. Y. *Cryst. Growth Des.* **2007**, *7*, 820.

(42) Ye, L.; Guo, W.; Yang, Y.; Du, Y. F.; Xie, Y. *Chem. Mater.* **2007**, *19*, 6331.

(43) Oaki, Y.; Imai, H. *Cryst. Growth Des.* **2003**, *3*, 711.

(44) Fukami, K.; Nakanishi, S.; Yamasaki, H.; Tada, T.; Sonoda, K.; Kamikawa, N.; Tsuji, N.; Sakaguchi, H.; Nakato, Y. *J. Phys. Chem. C* **2007**, *111*, 1150.

(45) Sunagawa, I. *Aquat. Sci.* **1993**, *55*, 347.

(46) Banga, D. O.; Vaidyanathan, R.; Liang, X. H.; Stickney, J. L.; Cox, S.; Happeck, U. Formation of PbTe Nanofilms by Electrochemical Atomic Layer Deposition (ALD). *58th Annual Meeting of the International Society of Electrochemisty*, Banff, Canada, 2007.

(47) Li, X. H.; Nandhakumar, I. S. *Electrochem. Commun.* **2008**, *10*, 363.

(48) Murphy, J. E.; Beard, M. C.; Norman, A. G.; Ahrenkiel, S. P.; Johnson, J. C.; Yu, P. R.; Micic, O. I.; Ellingson, R. J.; Nozik, A. J. *J. Am. Chem. Soc.* **2006**, *128*, 3241. Manciu, F. S.; Sahoo, Y.; Carreto, F.; Prasad, P. N. *J. Raman Spectrosc.* **2008**, *39*, 1135.

JP900452B